J. Am. Soc. Mass Spectrom. (2014) 25:790–799
DOI: 10.1007/s13361-014-0846-7

RESEARCH ARTICLE

Twelve Million Resolving Power on 4.7 T Fourier Transform Ion Cyclotron Resonance Instrument with Dynamically Harmonized Cell—Observation of Fine Structure in Peptide Mass Spectra

Igor A. Popov,[1,2,4] Konstantin Nagornov,[1] Gleb N.Vladimirov,[1,2] Yury I. Kostyukevich,[1,4] Eugene N. Nikolaev[1,2,3,4]

[1]Talrose Institute for Energy Problems of Chemical Physics of Russian Academy of Sciences, Moscow, Russia
[2]Emanuel Institute of Biochemical Physics of Russian Academy of Sciences, Moscow, Russia
[3]Orekhovich Institute of Biomedical Chemistry of Russian Academy of Medical Sciences, Moscow, Russia
[4]Moscow Institute of Physics and Technology, Dolgoprudny, Moscow Region, Russia

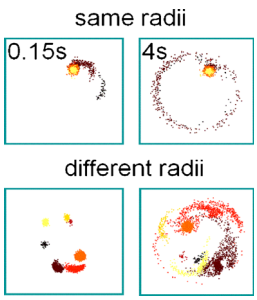

Abstract. Resolving power of about 12,000 000 at *m/z* 675 has been achieved on low field homogeneity 4.7 T magnet using a dynamically harmonized Fourier transform ion cyclotron resonance (FT ICR) cell. Mass spectra of the fine structure of the isotopic distribution of a peptide were obtained and strong discrimination of small intensity peaks was observed in case of resonance excitation of the ions of the whole isotopic cluster to the same cyclotron radius. The absence of some peaks from the mass spectra of the fine structure was explained basing on results of computer simulations showing strong ion cloud interactions, which cause the coalescence of peaks with *m/z* close to that of the highest magnitude peak. The way to prevent peak discrimination is to excite ion clouds of different *m/z* to different cyclotron radii, which was demonstrated and investigated both experimentally and by computer simulations.

Key words: FT-ICR, FTMS, Dynamic harmonization, Magnetic field, Ultra-high mass resolution, Simulation

Received: 8 October 2013/Revised: 28 January 2014/Accepted: 28 January 2014/Published online: 7 March 2014

Introduction

Fourier transform ion cyclotron resonance (FT ICR) mass spectrometry is widely used for identification of multiatomic molecules of different origin and for complex mixture analyses. It provides the highest mass accuracy and resolving power [1, 2]. In order to raise the resolution in FT ICR mass spectrometry higher than one million superconducting magnets with magnetic fields over 7 T are used [3–8]. It was recently demonstrated that an FT ICR cell with specially segmented and shaped excitation and detection electrodes provides harmonization of ion motion [9] and makes it possible to reach resolving power over 10 million on moderate 7 T magnetic field solenoids [5–7]. This allows resolving the fine structure of the isotopic peak distributions of molecules with masses of up to 5 kDa (insulin) using magnets with very high magnetic field homogeneity [10]. However, magnets with magnetic fields above 7 T are expensive to produce and to support their operation. These requirements limit the accessibility of FT ICR mass spectrometry. The high performance FTI CR mass spectrometry in peptide investigations is demonstrated using an unshielded 4.7 T magnet of very low magnetic field homogeneity and a laboratory prototype of dynamically harmonized ICR cell.

Further improvement of mass accuracy, sensitivity, dynamic range, and rate of spectra acquisition require deeper understanding of ion motion dynamics in ion formation, transfer, accumulation, and analyses devices. The most challenging problem is to take into account ion–ion interactions and their interactions with the electrodes via image charges. This problem becomes more pronounced by transition to high dynamic range mass spectrometry, when 10,000–50,000 components are identified in a single spectrum [11–13], and the number of ions in the FT ICR

Correspondence to: Eugene N. Nikolaev; *e-mail:* ennikolaev@rambler.ru

cell approaches 10 million. In this case, the electric field created by the ion ensemble is comparable to the electrostatic field created by the trapping electrodes [14]. Computer simulations [15–20] can be used to study the effects caused by ion–ion interactions: shifting of the measured frequency as a function of the number of ions in the clouds, coalescence[16], dephasing of ion cloud motion caused by cloud–cloud collisions [19], and ion cloud stabilization (condensation) [15, 16, 19]. Most of these effects depend on magnetic field strength and become more pronounced at lower fields. In this work, we provide experimental results accompanied by computer simulations on the destruction of smaller ion clouds by bigger ion clouds, which leads to the disappearance of some peaks in the spectrum of low Tesla FT ICR instruments, and the influence of the cyclotron frequency excitation modes on this effect.

Recently, it has been demonstrated by Marshall et al. on a 9.4 T FT-ICR instrument that excitation of different *m/z* ion clouds to different cyclotron radii results in a 3-fold increase in the dynamic range in case of complex mixture analyses [13]. In this work, we show an improvement in the dynamic range (more peaks in the fine structure mass-spectra of peptides), when we use off-resonance single frequency excitation, which excites different *m/z* ions to different orbits.

Experimental

FT ICR Instruments

FT ICR mass spectra were acquired using a Bruker Apex Qe mass spectrometer (Bruker Daltonics, Billerica, MA, USA) equipped with an unshielded 4.7 T Bruker BZH 200/150 magnet (Oxford Instruments, Abingdon, UK) and a Bruker Apollo API ion source (Bruker Daltonics, Billerica, MA, USA). Shimming of the magnet was unbalanced. The magnetic field homogeneity was evaluated experimentally by moving the mass spectrometer with the ICR cell along the magnet axis and measuring the detected signals – reduced cyclotron frequency of the selected ions, ν_+. These signals were measured for the isotopes of the doubly charged ion of the angiotensin I peptide produced by electrospray ionization in the "high resolution" mode. Figure 1 shows the axial and radial field inhomogeneities of the magnet. The magnetic field axial inhomogeneity was about 800 ppm along 8 cm for the 1 cm radius cylinder (excitation to 1 cm cyclotron radius). The radial inhomogeneity in the range of cell radii $\Delta R = 0.02 \div 2.2$ cm was measured. The cyclotron frequency varied in the range $\Delta\nu_+ = \pm 0.4$Hz for post excitation radii of $\Delta R_{exc} = 0.2 \div 2.2$ cm, so the radial inhomogeneity was less than 2 ppm along 2 cm. The significant decrease of the cyclotron frequency at the small radius R = 0.02 cm occurred because of the influence of ion–ion interactions [21].

The ions were accumulated in the source hexapole and then ejected with a 1.5 V offset voltage into the FT ICR cell through an analytical quadrupole and through the ion transfer optics system. The analytical quadrupole was employed in the isolation mode with a $2 \div 4$ Da isolation window. The optimal ion transfer time between the source hexapole and the ICR cell for the ions in the *m/z* range from 400 to 700 was about 2 ms. Measurements were carried out without preliminary cooling of the ion translational motion in the collision cell or directly in the ICR cell. FT ICR signals were acquired using single-frequency excitation ("shot" mode) of the ion cyclotron motion followed by heterodyne detection in the $0.5 \div 1.0$ Da mass range and magnitude mode Fourier transform without apodization. It was found that summing of several scans leads to the decrease in resolving power because of the frequency drift between scans. Thus, all of the presented mass spectra were obtained for single data acquisition periods.

A laboratory prototype of the dynamically harmonized ICR cell (cylindrical, 56-mm i.d. and 150 mm long) was used [5–7, 9]. The selected ions were confined in the cell during excitation/detection events by the static trapping potentials: $V_{trap} = 4.10$ V on the entrance plate and $V_{trap} = 3.00$ V on the back plate. The distinction between the trapping potentials (with accuracy of 0.01 V) was crucial to achieve high FT ICR performance as will be explained below.

In order to improve the dynamic range of the harmonized cell off-resonance excitation was used. Equation 1 (taken from [1]), shows that a long single-frequency excitation with low excitation amplitude can excite ions with close cyclotron frequencies to different cyclotron radii:

$$R_{exc} = \frac{\beta_{dipolar}}{2dB} \cdot \frac{U_0 \cdot \sin(2\pi(\nu_{exc} - \nu_+) \cdot T_{exc})}{2\pi(\nu_{exc} - \nu_+)} \quad (1)$$

where $\beta_{dipolar}$ is the scaling factor, d is the diameter of the trap, B is the magnetic field magnitude. Figure 2 shows off-resonance single-frequency excitation variations examined in this work for doubly protonated Substance P ions. For example, in the case (1) of Figure 2, ions whose reduced cyclotron frequencies are in the range $\Delta\nu_+ = \pm 500$ Hz [~(670–680) *m/z* for 4.7 T], relative to the excitation frequency, would be excited to nearly the same post-excitation radii, and in case (3), the ions even from the range $\Delta\nu_+ = \pm 3$ Hz would be excited to significantly different post-excitation radii.

Simulation Method

In the present computer simulations we have used a previously developed computer code based on the Particle-in-Cell algorithm for calculating the electric forces acting on an individual ion from other ions in the cloud, from the field on the electrodes, and from image charges of these electrodes [7, 15–20]. Briefly, the whole space occupied by the cell was subdivided by a mesh. The ion density distribution was determined at

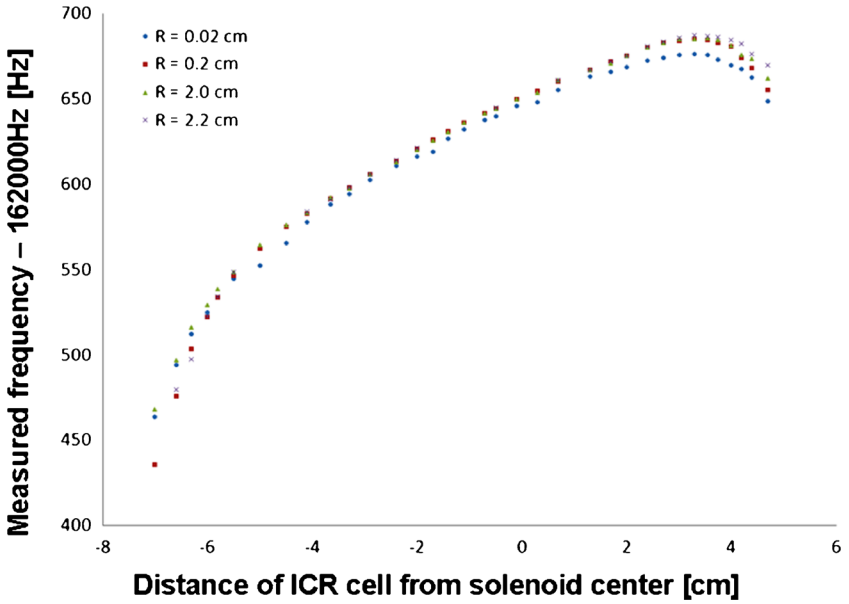

Figure 1. Axial and radial magnetic field distribution for Bruker BZH 200/150 magnet. The measured cyclotron frequency as a function of the relative distance between the ICR cell and the solenoid center in the –8 to +6 cm region. For the radial homogeneity estimation, the FT ICR signal was measured at the different radii of ion cyclotron motion

every node of the mesh by dividing the total charge extrapolated to that particular node by the number of ions in the volume of each elementary cube of the mesh. By using the direct fast Fourier transform (FFT) Poisson solver with the trap's boundary conditions, corresponding to DC and rf potentials on the trap electrodes, the charge density on each grid point was converted into the potentials at those points, and the electric field was determined from the spatial derivatives of the potentials. The electric field at an individual ion position was calculated by interpolating the electric fields from the nearest grid points based on the same weighting algorithm as for the charge projections to each grid point. The mathematical description of the whole procedure for solving the Poisson equation by the FFT method is described in [15, 22]. The particle positions

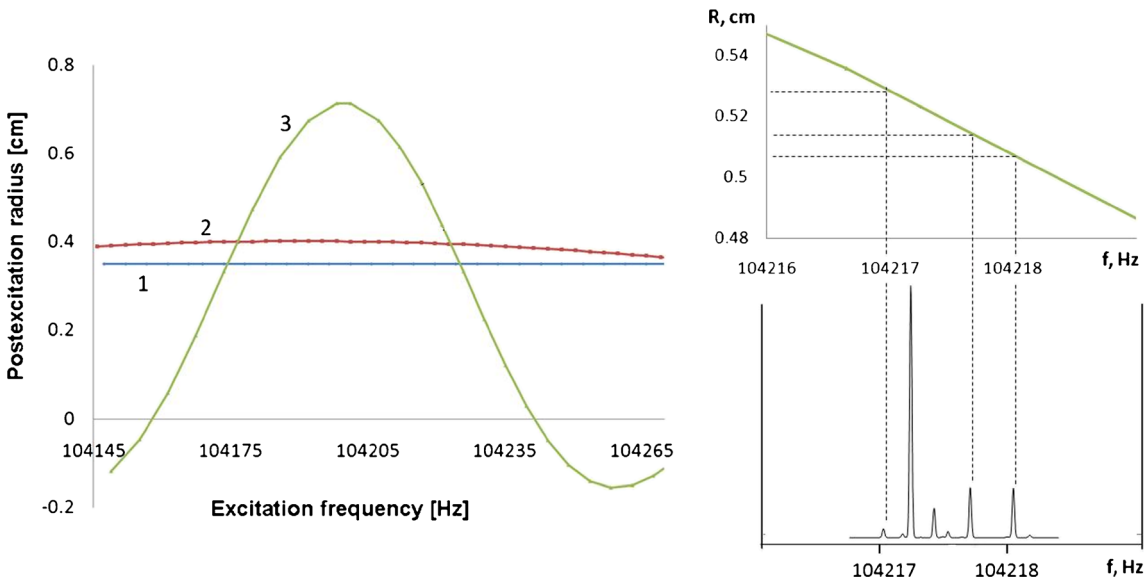

Figure 2. Dependence of the post-excitation cyclotron radius of the isotope cluster fine structure of Substance P ions on the excitation frequency offset, for different dipolar excitation parameters (left): (1) U_0 = 12 V, T_{exc} = 0.14 ms; (2) U_0 = 1.8 V, T_{exc} = 1.5 ms; (3) U_0 = 0.4 V, T_{exc} = 12.0 ms. Selected ions of the fine structure of the isotope cluster were excited to different radii (right) for U_0 = 0.4 V, T_{exc} = 12.0 ms

and velocities for the next time-step were calculated with the Boris integrator [22]. For the traps that have a non-cubic geometry, the electric field created by the electrodes was calculated by solving the Laplace equation using the relaxation method in the SIMION program [23]. The electric field from the ions has been determined by solving the Poisson equation using the particle-in-cell (PIC) method with zero voltages on the electrodes of a cubic trap. Then, in accordance with the superposition principle these two fields were summed together to obtain the total electric field. This was done because the PIC method does not work well for non-cubic cells. For the simulation we used 64 × 64 × 64 PIC grids for a 50.8 × 50.8 × 50.8 mm cell with a hyperbolic potential. For the cell with dynamic harmonization a 150 × 150 × 350 SIMION mesh was used, which corresponds to a 75 mm × 75 mm × 175 mm simulation region (trap length 152 mm, trap diameter 60 mm). The number of time steps in the minimal cyclotron period was 100 for all simulations. The number of stored snapshots per simulation was determined from the snapshot repetition rate, namely, after every 100,000 steps. The CUDA programming interface was used to implement part of the simulation on the GPU. Simulations were performed on a homebuilt PC with 24 GB ram and two GTX 580 GPU.

Results and Discussion

A time-domain transient detection signal of about 180 s in duration and resolution – 12,000,000 at *m/z* 675 were experimentally achieved for the doubly protonated Substance P peptide (Figure 3a), using an FT ICR instrument described above. We are measuring the resolving power as full width at half maximum (FWHM) of individual peak. The theoretical resolution corresponding to a 180 s duration of an undamped ICR signal is about 18,000,000 in accordance with the expression for FT CR resolution as a function of the observation period. The difference between the theoretical and measured resolution values for the current signal is explained by the drift of the cyclotron frequency during the detection sequence due to ion-ion interactions at the relatively small post excitation radius R_{exc} = 0.4 cm. The magnitude of the frequency drift during detection was about $\Delta\nu_+$ = +0.0085 Hz and corresponds to the measured resolution value at the current cyclotron frequency of 104.2 kHz.

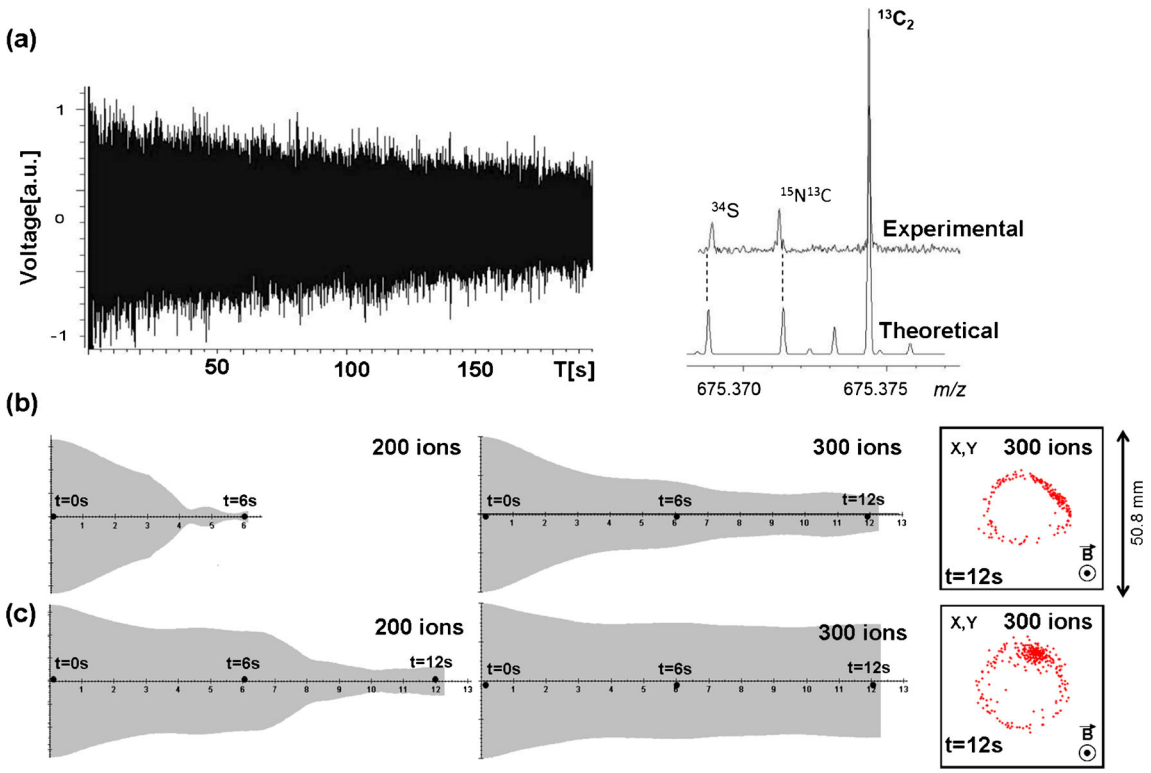

Figure 3. **(a)** Experimental time-domain (left) signal and magnitude-mode Fourier transform (right) mass spectrum for doubly protonated Substance P isotope cluster $^{13}C_2$. Selected ions were excited to nearly the same-post excitation cyclotron radii R_{exc} = 0.4 cm. Detection mass range 0.5 Da; **(b)** and **(c)** signals obtained by computer simulation and x-y projection of ion clouds: **(b)** - no compensation, **(c)** - with compensated Z^1Z^2 components of the inhomogeneous magnetic field [10]. Data for the inhomogeneous magnetic field was taken for Spectrospin AG magnet description [25], B = 4.7 T, the axial inhomogeneity - 10 ppm along 1 cm, *m/z* = 500 Da, Z = 1 e

For ideal time domain signal in FT ICR MS resolving power is proportional to the duration of ions' synchronous motion, which depends on ion trap geometry and magnetic field homogeneity. It is well known that during excitation and detection, ions oscillate axially in the direction parallel to the magnetic field and the cyclotron and magnetron frequencies in an FT ICR cell without harmonization depend significantly on the axial oscillation amplitude and magnetic field magnitude. Synchronous ion motion should be rapidly dephased in highly axialy inhomogenic magnetic field and the ICR signal should be lost [7, 15, 16, 19]. This does not happen at relatively large numbers of ions in the cell because of the so-called "phase locking." As we know from realistic supercomputer modelling [7, 19, 24], we should distinguish two mechanisms of phase locking. The first one is the so-called "condensation" mechanism (a magnetic field-independent phenomenon), when ions of the same *m/z* become phase locked by equalizing their axial oscillation amplitudes and by this their magnetron frequencies. The second one is coallescence (a magnetic field-dependent phenomenon), when ions stick to each other via magnetron type rotation around each other caused by Coulomb interections between them. The first phenomenon prevents comet formation in ion clouds of the same *m/z* and allows long signal durationss even in non-ideal electric trapping fields (that is why we see an FT ICR signal at all in conventional cubic or cylindrical cells). The peak coalescence phenomenon is easy to observe experimentaly. It manifests itself through merging of close *m/z* peaks into one narrow peak. This phenomenon that leads to the coalescence of peaks with different *m/z* ratios also exists for ions with the same *m/z*. This results in more pronounces phase locking and long signal durations up to 10–100 s even in cells with a non-ideal electric trapping fields. So, when the number of ions in a cell reaches coalescence conditions, we can get a very long time-domain signal and narrow individual peaks in the spectra, formaly giving us the resolving power of over one million, but with such resolution we are not resolving close peaks, we are killing them by merging close *m/z* ion clouds or by destroying the phase synchronization of ions in these clouds. Results of the simulations show that ion cloud dephasing and "comet" structure formation at small amount of ions in the cell can be prevented by compensating the magnetic field's Z^1Z^2 components [10] and increasing the number of ions in the ion cloud participating in the detection event (Figure 3b, c). It was mentioned above that ions were confined by unequal trapping potentials. Fine adjustment of the difference beetween the traping potentials compensated the axial magnetic field inhomogeneity. It allowed us to obtain long time domain ICR signals, over 100 s, using the dynamically harmonized cell even for lowly homogenic magnetic field. The amount of ions participating in detection was also crucial for experimental long time domain signals achievement.

It is clear that the optimal compensation voltage for magnetic induction inhomogeneity is mass-dependent [10]. However, because of ion cloud condensation phenomenon compensation of magnetic field inhomogenity operates in a

Table 1. Resolving Power Obtained Using Different FT-ICR Instruments

	FT-ICR instrument details	Sample	*m/z* [Da/e]	m[Da]	Resolving Power	M/ΔM for the closest peaks	References
1	1 T; cylindrical cell	Bradykinin	~531	~1060	1.4 10^6; C^{13} cluster resolved	~1000	[29]
2	3 T; cylindrical cell with segmented trapping electrodes	Melittin	~713	~2846	0.4 10^6; C^{13} cluster resolved	~2800	[26]
3	4.7 T (low homogenity); dynamically harmonized cell	Substance P	~675	~1347	12 10^6; fine structure resolved	~0.55 10^6 675.37347 and 675.37470	
4	7 T; cylindrical cell with multi-electrode detection (2ω+)	132Xe+	~132	~132	211 10^6; single peak		[31]
5	7 T; cylindrical cell with compensation electrodes	Vasopressin	~1084	~1084	17 10^6 ; single peak		[27]
6	7 T; dynamically harmonized cell	Reserpine	~609	~609	39 10^6; single peak		[7, 30]
7	7 T; dynamically harmonized cell	Reserpine	~609	~609	1.3 10^6; fine structure resolved	~1.5 10^6 613.294939 and 613.294535	[6]
8	7 T; dynamically harmonized cell	Substance P	~675	~1347	6 10^6; fine structure resolved	~1.5 10^6 675.37514 and 675.3747	[5, 30]
9	7 T; dynamically harmonized cell	Insulin	~956	~5808	5 10^6 ; fine structure resolved	~2.45 10^6 956.60861 and 956.609	[30]
10	7 T; dynamically harmonized cell	Bovine serum albumin	~1303	~66420	1.7 10^6; C^{13} cluster resolved	~66000 1303.44092 and 1303.46059	[30]
11	7 T; dynamically harmonized cell	Enolase tetramer	~5834	~186660	0.4 10^6; C^{13} cluster resolved	~186000	[7, 30]
12	9.4 T; large-diameter (D = 10 cm) cylindrical cell	Bovine Insulin	~1147	~5730	5 10^6; fine structure resolved	~2.3 10^6 1147.93069 and 1147.93118	[3]
13	9.4 T; large-diameter (D = 10 cm) cylindrical cell	Bovine Ubiquitin	~952	~8560	8 10^6; fine structure resolved		[3]
14	9.4 T; large-diameter (D = 10 cm) cylindrical cell	$C_{35}H_{68}N_{16}O_8S_2$ and $C_{35}H_{60}N_{20}O_9$	~453	~906	3 10^6; doublet resolved	~3 10^6 904.4847 and 904.485	[32]
15	9.4 T; large-diameter cylindrical cell with compensation electrodes	IgG1k	~2593	~147664	0.4 10^6; C^{13} cluster resolved	~150000	[28]

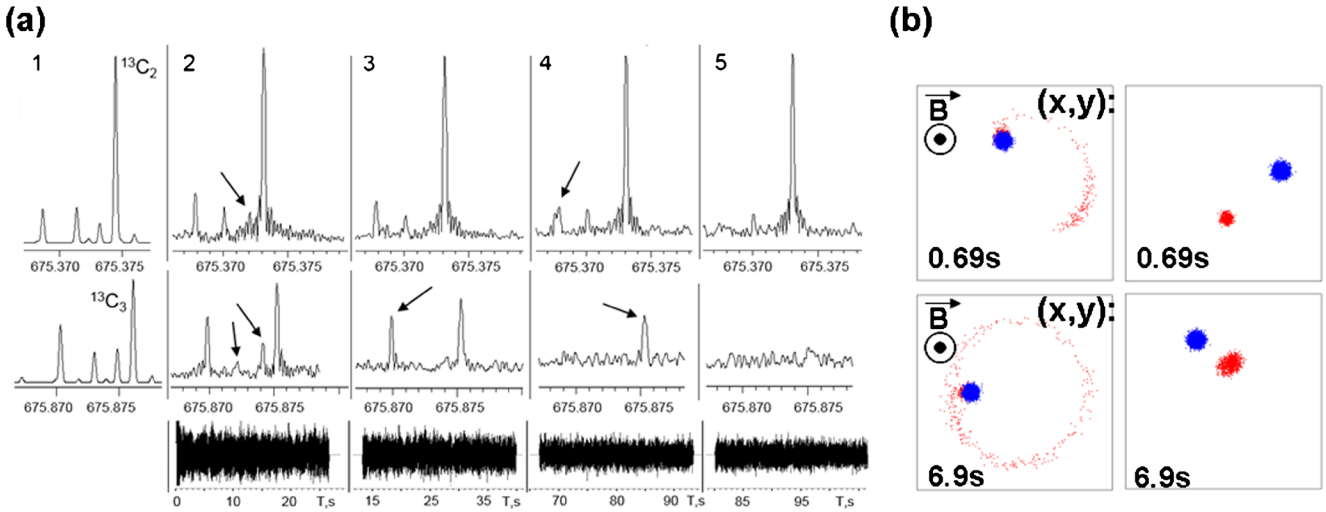

Figure 4. **(a)** Experimental mass-spectra and time domain signals of Substance P $^{13}C_2$ and $^{13}C_3$ isotopes fine structure of doubly charged molecular ions for detection time 106 s; (1 - theoretical, 2–5 - experimental). Signals (2–5) were measured for 27 s "time-windows" (different parts of the full signal). Selected ions were excited to nearly the same post-excitation cyclotron radii R_{exc} = 0.4 cm. The detection mass range of 1 Da covers both isotopic distributions. **(b)** PIC-simulation results for ion clouds excited to equal radii (left) and different radii (right): (x,y) projectionss; 675.36925 *m/z*, 1000 ions = red cloud; 675.37470 *m/z*, 10,000 ions = blue cloud; B = 4.7 T

rather broad *m/z* window (when optimum *m/z* for compensation is set to be 500 Da at 5 Tesla, compensation window is covering 400–900 Da window) [24].

Long time domain signals were obtained by other groups using conventional cylindrical cells and so-called compensated cells, in which a hyperbolic-like or flat potential is formed by inserting additional segments to the trapping [26] or detection-excitation electrodes of a regular cylindrical cell [27, 28]. Results obtained by these groups are summarized in Table 1. The resolving power claimed by these groups was measured like in our case as FWHM and individual peaks were used for its determination. FWHM definition does not give us the real resolving power in case of FT ICR MS because of the above-mentioned reason that we could have coalescence (see Table 1 lines 6 and 7) of close peaks as has been noted by Marshall's group [32]. So, the resolving power of 1 million on an isolated peak will not guarantee that we can resolve a doublet separated by a Δm of one millionth part of m. The correct way to measure resolving power in FT ICR MS is to use not a single peak but a doublet or a multiplet. For this reason, it is difficult to compare the results of different groups (except for Marshall's group) because they do not present close doublets or even fine structures. It is very likely that long signal duration is the result of coalescence. As was pointed out in [33] "…phase locking of an ion cloud that contains ions of the same *m/z* results in artificially lower peak widths. In the limit, where all ions with the same *m/z* have the same frequency regardless of mode amplitude, one cannot distinguish between an ion cloud that is phase locked and one that is not…"

The possibility to resolve close doublets is critical for investigation of complex mixtures [11, 13] and for conducting isotopic exchange experiments [35, 36].

It should be noted that a significant number of peaks were absent from the mass spectrum of the fine structure of the isotopic distribution of Substance P in case of nearly same radii of ion cyclotron motion [Figure 3a (right)]. The disappearance of peaks from the fine structure is caused by the interactions of ion clouds [7, 19]. Ion clouds of different (though close) *m/z* pass through each other during their cyclotron motion, and ion clouds that contain small numbers of ions get scattered by the clouds with high numbers of ions or the become stuck to them (coalescence) [15, 16]. The last phenomenon is more essential for the closest peaks in the fine structure: for example, absence of peak 675.3747 from the fine structure of 7 T FT-ICR mass-spectra of Substance P $(M + 2H)^{+2}$ could be explained by coalescence [19]. Such ion cloud dissipation effect (and hence the disappearance of peaks from the mass spectra) is significant for the long duration FT ICR signals, as the number of ion cloud passages through each other increases with the detection

Table 2. PIC Computer Simulation Data (Calculated using [34])

	Substance P (third cluster)$^{+2}$		Angiotensin I (third cluster)$^{+3}$	
	m/z, Da	Ion abundance, pcs.	*m/z*, Da	Ion abundance, pcs.
1	675.36838	20	433.5644226	54
2	675.36925	330	433.5665283	1272
3	675.37154	330	433.5674744	24
4	675.37272	40	433.5678101	840
5	675.37347	190	433.568634	7017
6	675.37470	1680	433.5689087	117
7	675.37514	25	433.5695801	276
8	675.37617	50	–	–

time increment. In order to study this phenomenon, we have carried out a series of FT ICR experiments and computer simulations. The experimental FT ICR signal, 106 s in duration with a 1 Da detection mass range, which covered the $^{13}C_2$ and $^{13}C_3$ isotopes of the +2 charge state of Substance P, was cropped to 27 s time segments at different points; the most informative of them in proper sequence are represented on Figure 4a. The selected ions were excited to nearly the same post-excitation radii using the off-resonance dipolar excitation [(1) on Figure 2] described in the Experimental section. The results of the FT ICR experiments have shown that the peaks, which correspond to ion clouds with the smallest number of ions dissapear earlier—already at the beginning of the detection period [Figure 4a (2), (3)], whereas peaks corresponding to clouds containing a bit more of ions disappear little bit later [Figure 4a (4)]. The results of the simulation show that after an ion cloud that contains 1000 elementary charges passes by an ion cloud with the number of charges on the order of 10,000, the initially close phases of cyclotron motion of ions in the first cloud get significantly distorted (Figure 4b). Thus, the considered phenomenon is caused by ion–ion interactions, which leads to limitations in resolving power and dynamic range [7, 24].

The phenomenon of small ion cloud destruction by bigger ones with close *m/z* ratios could be prevented by exciting ions with different *m/z* to different radii of cyclotron motion (Figure 4b). In order to prove this hypothesis, a series of FT ICR experiments and computer simulations have been carried out. Experimental and simulated fine structure distributions of Substance P and angiotensin I obtained by exciting ions to the same and different radii were compared. Ions of the +2 charge state of Substance P were excited to different radii by using dipolar amplitude excitation, U_0 = 0.4 V, for a period of T_{exc} = 12 ms, and a frequency offset, $\nu_{exc}-\nu_+$ = 20Hz, relative to the measured reduced cyclotron frequency of the selected ions (3 Figure 2b). For the same measurements with angiotensin I, the following excitation parameters were applied: U_0 = 0.2 V, T_{exc} = 25 ms, $\nu_{exc}-\nu_+$ = 3 Hz. Table 2 shows the number of ions of Substance P and angiotensin I used to implement the PIC simulations.

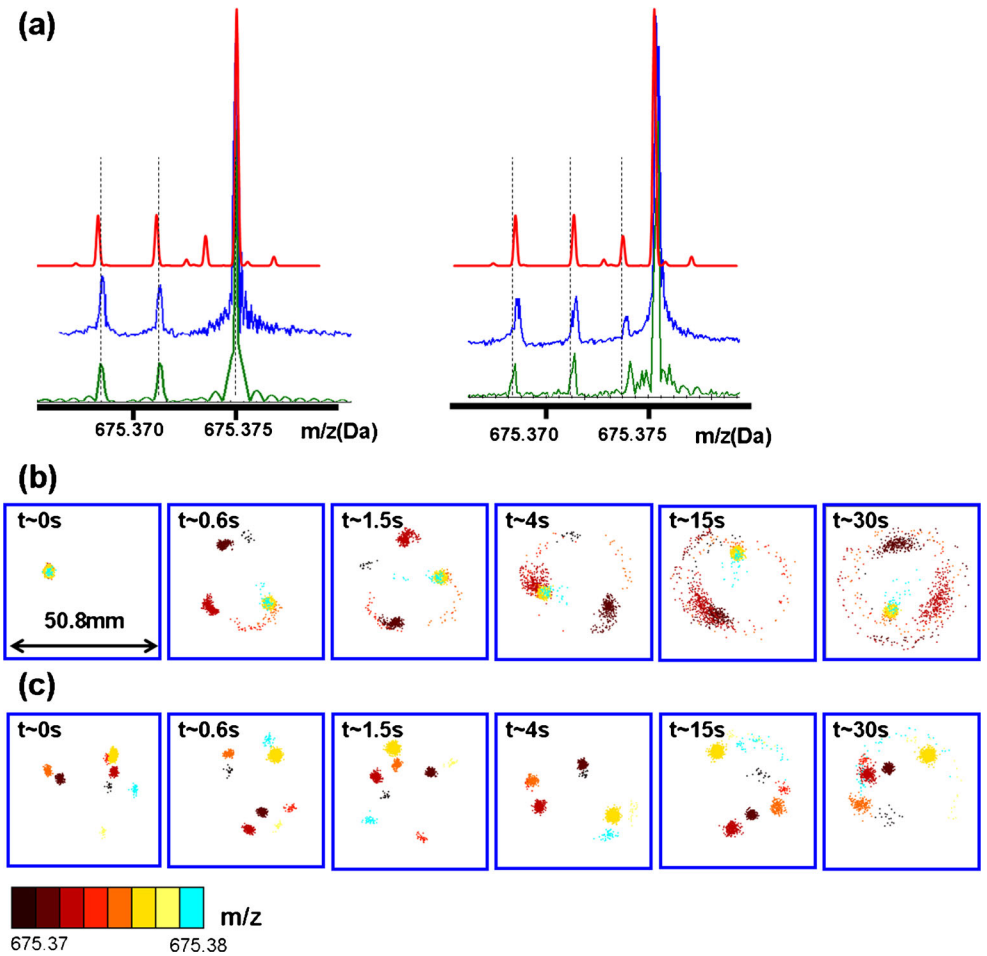

Figure 5. **(a)** Fine structure of the $(M + 2H)^{2+}$ of Substance P (C63H98N18O13S1 + 2H) at 4.7 T; second 13C isotopic cluster: (top, red) - theoretical for T_{det} = 100 s; (middle, blue) - experimental, T_{det} = 40s; (bottom, green) - PIC simulations, T_{det} = 30s; (left) ion clouds on equal orbits; (right) ion clouds on different orbits; **(b)** x-y projections of ion clouds dynamic-excited to equal radii; **(c)** x-y projections of the ion clouds excited to different radii

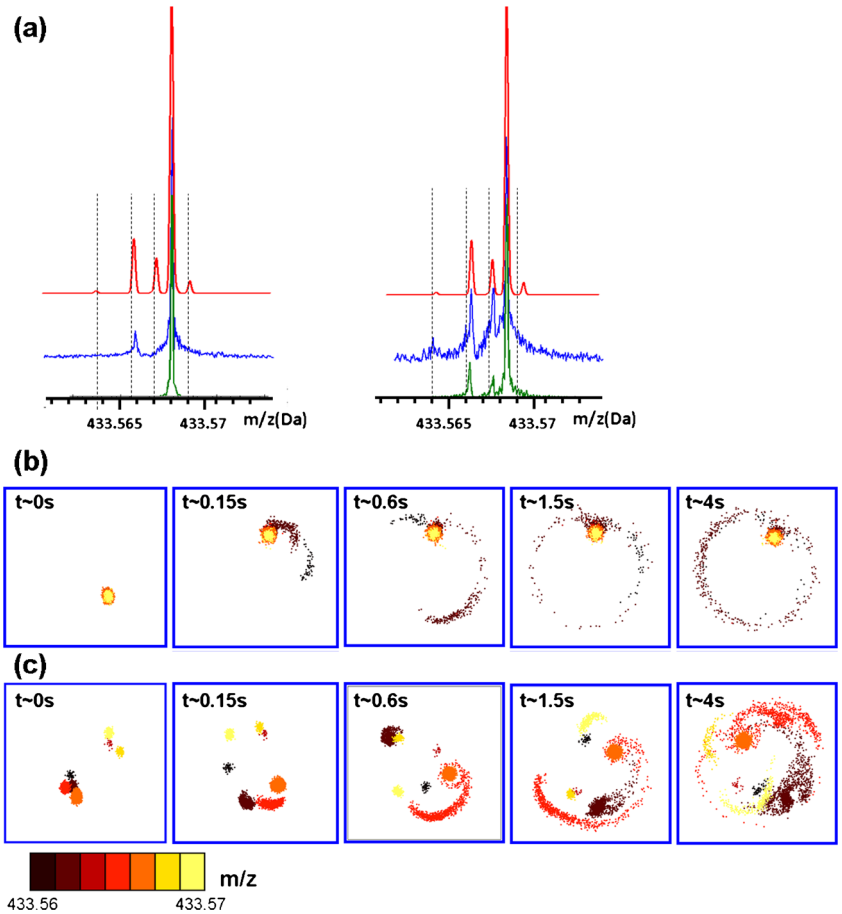

Figure 6. **(a)** Fine structure of the $(M + 3H)^{+3}$ of angiotensin I ($C_{62}H_{89}N_{17}O_{14} + 3H$) mass-spectra at 4.7 T, third 13C isotopic cluster: (top, red) - theoretical, T_{det} = 60 s; (middle, blue) - experimental, T_{det} = 40 s; (bottom, green) - PIC simulation, T_{det} = 60 s; (left) ion clouds on equal orbits; (right) ion clouds on different orbits; **(b)** x-y projections of the ion clouds excited to equal radii; **(c)** x-y projections of the ion clouds excited to different radii

The experimental and computer simulations results (Figures 5 and 6) demonstrate the appearance of the corresponding peaks in the mass spectra (which were present in the theoretical spectra) in the case if different *m/z* ions have different cyclotron radii during the detection event. It can be noted that experimental and simulated results are in good agreement with each other.

However, some peaks in the mass spectra corresponding to ion clouds with the smallest ion abundances were still not observed because of their dissipation by bigger ion clouds. A possible way to resolve more peaks in the mass spectra was to increase the difference between ions motion radii. However, this just led to a significant discrimination of peaks corresponding to ion clouds rotating at smaller cyclotron radii while additional peaks did not appear, since the FT ICR signal magnitude depends on cyclotron ion motion radius linearly [1]. Other possible ways to resolve more peaks are to reduce the ion abundance and to improve the magnetic field homogeneity. It has been demonstrated that the use of high magnetic field 7 T of very high homogeneity allows resolving more peaks of the isotopic fine structure of Substance P [7, 24].

Conclusions

An 180 s time transient detection signal and resolving power (HWHM, of isolated peak) of 12,000,000 were experimentally achieved for the doubly protonated Substance P peptide (in conditions of observation fine structure in its mass spectrum) using an FT ICR instrument equipped with an unshielded 4.7 T superconducting magnet with a very high axial inhomogeneity. The resolving power for these measurements was limited by cyclotron frequency drift during the detection event. Compensation of the magnetic field's Z^1Z^2 components by fine-tuning the trapping potential for each end plate separately enables generation of highly resolved ICR signals even for a low homogeniety magnetic field. Some of the peaks present in the theoretical spectrum were not observed in the mass spectra obtained experimentally and by PIC simulation

on occasion of equal ion rotation radii. The ion cloud dissipation effect and, hence, the disappearance of peaks from the mass spectra is caused by ion–ion interactions, which leads to certain limitations in resolving power and dynamic range. Excitation of ions with different *m/z* to different radii of cyclotron motion using off-resonance single frequency excitation allows avoiding the phenomenon of small ion cloud destruction by bigger clouds with close *m/z* ratios.

Acknowledgments

The authors acknowledge the support from the Russian Foundation of Basic Research (grants 12-08-31460, 13-04-40110-n-komfi, 13-08-01445-a, 14-08-01236-a, 14-08-31652-mol-a, 14-08-31360-mol-a), Bruker Company, and from the Ministry of Science and Education (grant 8149, 8153). The authors gratefully acknowledge Maria I. Indeykina for her comments of various aspects of this work.

References

1. Marshall, A.G., Hendrickson, C.L., Jackson, G.S.: Fourier transform ion cyclotron resonance mass spectrometry: a primer. Mass Spectrom. Rev. **17**(1), 1–35 (1998)
2. Marshall, A.G.: Milestones in Fourier transform ion cyclotron resonance mass spectrometry technique development. Int. J. Mass Spectrom. **200**(1), 331356 (2000)
3. Shi, S.D.H., Hendrickson, C.L., Marshall, A.G.: Counting individual sulfur atoms in a protein by ultrahigh resolution Fourier transform ion cyclotron resonance mass spectrometry: experimental resolution of isotopic fine structure in proteins. Proc. Natl. Acad. Sci. **95**(20), 11532–11537 (1998)
4. Gorshkov, M.V., Paša Tolić, L., Udseth, H.R., Anderson, G.A., Huang, B.M., Bruce, J.E., Priora, D.C., Hofstadler, S.A., Tang, L., Chen, L.-Z., Willetta, J.A., Rockwood, A.L., Sherman, M.S., Smith, R.D.: Electrospray ionization–Fourier transform ion cyclotron resonance mass spectrometry at 11.5 tesla: instrument design and initial results. J. Am. Soc. Mass Spectrom. **9**(7), 692–700 (1998)
5. Nikolaev, E.N., Boldin, I.A., Jertz, R., Baykut, G.: Initial experimental characterization of a new ultra-high resolution FT ICR cell with dynamic harmonization. J. Am. Soc. Mass Spectrom. **22**(7), 1125–1133 (2011)
6. Nikolaev, E.N., Jertz, R., Grigoryev, A., Baykut, G.: Fine structure in isotopic peak distributions measured using a dynamically harmonized Fourier transform ion cyclotron resonance cell at 7 T. Anal. Chem. **84**(5), 2275–2283 (2012)
7. Nikolaev, E.N., Vladimirov, G.N., Jertz, R., Baykut, G.: From supercomputer modeling to highest mass resolution in FT-ICR. Mass Spectrom (Tokyo), 2(Spec Iss). S0010 (2013), http://www.ncbi.nlm.nih.gov/pmc/articles/PMC3810098/
8. Miura, D., Tsuji, Y., Takahashi, K., Wariishi, H., Saito, K.: A strategy for the determination of the elemental composition by Fourier transform ion cyclotron resonance mass spectrometry based on isotopic peak ratios. Anal. Chem. **82**(13), 5887–5891 (2010)
9. Boldin, I.A., Nikolaev, E.N.: Fourier transform ion cyclotron resonance cell with dynamic harmonization of the electric field in the whole volume by shaping of the excitation and detection electrode assembly. Rapid Commun. Mass Spectrom. **25**(1), 122–126 (2011)
10. Kostyukevich, Y.I., Vladimirov, G.N., Nikolaev, E.N.: Dynamically harmonized FT-ICR cell with specially shaped electrodes for compensation of inhomogeneity of the magnetic field. Computer simulations of the electric field and ion motion dynamics. J. Am. Soc. Mass Spectrom. **23**(12), 2198–2207 (2012)
11. Hughey, C.A., Rodgers, R.P., Marshall, A.G.: Resolution of 11,000 compositionally distinct components in a single electrospray ionization Fourier transform ion cyclotron resonance mass spectrum of crude oil. Anal. Chem. **74**(16), 4145–4149 (2002)
12. Schaub, T.M., Hendrickson, C.L., Horning, S., Quinn, J.P., Senko, M., Marshall, A.G.: High-performance mass spectrometry: Fourier transform ion cyclotron resonance at 14.5 Tesla. Anal. Chem. **80**(11), 3985–3990 (2008)
13. Kaiser, N.K., McKenna, A.M., Savory, J.J., Hendrickson, C.L., Marshall, A.G.: Tailored ion radius distribution for increased dynamic range in FT ICR mass analysis of complex mixtures. Anal. Chem. **85**(1), 265–272 (2012)
14. Mitchell, D.W., Smith, R.D.: Cyclotron motion of two Coulombically interacting ion clouds with implications to Fourier transform ion cyclotron resonance mass spectrometry. Phys. Rev. E. **52**(4), 4366 (1995)
15. Nikolaev, E.N., Heeren, R., Popov, A.M., Pozdneev, A.V., Chingin, K.S.: Realistic modeling of ion cloud motion in a Fourier transform ion cyclotron resonance cell by use of a particle-in-cell approach. Rapid Commun. Mass Spectrom. **21**(22), 3527–3546 (2007)
16. Vladimirov, G., Hendrickson, C.L., Blakney, G.T., Marshall, A.G., Heeren, R.M., Nikolaev, E.N.: Fourier transform ion cyclotron resonance mass resolution and dynamic range limits calculated by computer modeling of ion cloud motion. J. Am. Soc. Mass Spectrom. **23**(2), 375–384 (2012)
17. Leach III, F.E., Kharchenko, A., Heeren, R., Nikolaev, E., Amster, I.J.: Comparison of particle-in-cell simulations with experimentally observed frequency shifts between ions of the same mass-to-charge in Fourier transform ion cyclotron resonance mass spectrometry. J. Am. Soc. Mass Spectrom. **21**(2), 203–208 (2010)
18. Leach III, F.E., Kharchenko, A., Vladimirov, G., Aizikov, K., O'Connor, P.B., Nikolaev, E., Heeren, R., Amster, I.J.: Analysis of phase dependent frequency shifts in simulated FTMS transients using the filter diagonalization method. Int. J. Mass Spectrom. **325**, 19–24 (2012)
19. Nikolaev, E.N., Vladimirov, G., Boldin, I.A.: Influences of non-neutral plasma effects on analytical characteristics of the top instruments in mass spectrometry for biological research. AIP Conf. Proc. **1521**, 281 (2013)
20. Kharchenko, A., Vladimirov, G., Heeren, R.M., Nikolaev, E.N.: Performance of Orbitrap mass analyzer at various space charge and non-ideal field conditions: simulation approach. J. Am. Soc. Mass Spectrom. **23**(5), 977–987 (2012)
21. Gorshkov, M.V., Nikolaev, E.N.: Optimal cyclotron radius for high resolution FT ICR spectrometry. Int. J. Mass Spectrom. Ion Process **125**(1), 1–8 (1993)
22. Hockney, R.W., Eastwood, J.W.: Computer simulation using particles. Adam Hilger, New York (1988)
23. Dahl, D.A.: SIMION for the personal computer in reflection. Int. J. Mass Spectrom. **200**(1), 3–25 (2000)
24. Nikolaev, E.N., Kostyukevich, Y.I., Vladimirov, G.N.: Fourier transform ion cyclotron resonance (FT ICR) mass spectrometry: Theory and simulations. Mass Spectrom. Rev. (2014). doi:10.1002/mas.21422
25. Laukien, F.H.: The effects of residual spatial magnetic field gradients on Fourier transform ion cyclotron resonance spectra. Int. J. Mass Spectrom. Ion Process **73**(1), 81–107 (1986)
26. Weisbrod, C.R., Kaiser, N.K., Skulason, G.E., Bruce, J.E.: Trapping ring electrode cell: A FT ICR mass spectrometer cell for improved signal-to-noise and resolving power. Anal. Chem. **80**(17), 6545–6553 (2008)
27. Brustkern, A.M., Rempel, D.L., Gross, M.L.: An electrically compensated trap designed to eighth order for FT-ICR mass spectrometry. J. Am. Soc. Mass Spectrom. **19**(9), 1281–1285 (2008)
28. Valeja, S.G., Kaiser, N.K., Xian, F., Hendrickson, C.L., Rouse, J.C., Marshall, A.G.: Unit mass baseline resolution for an intact 148 kDa therapeutic monoclonal antibody by Fourier transform ion cyclotron resonance mass spectrometry. Anal. Chem. **83**(22), 8391–8395 (2011)
29. Gorshkov, M.V., Udseth, H.R., Anderson, G.A., Smith, R.D.: High performance electrospray ionization Fourier transform ion cyclotron resonance mass spectrometry at low magnetic field. Eur. J. Mass Spectrom. **8**(2), 169–176 (2002)
30. Nikolaev E.N.: The way to isotopic resolution of mega-Dalton protein mass spectra for top-down proteomics. Proceedings of the 61th ASMS Conference on Mass Spectrometry and Allied Topics, Minneapolis, June 9–13, WOE am 08:30 (2013)

31. Knobeler, M.; Wanczek, K.P.: Detection of harmonic and multiples of the fundamental frequency in Fourier transform ion cyclotron resonance mass spectrometry. Proceedings of the ASMS Conference on Mass Spectrometry and Allied Topics, Palm Springs, CA, USA, June 1–5 Session: Trapped ions: FT ICR – 079 (1997)
32. He, F., Hendrickson, C.L., Marshall, A.G.: Baseline mass resolution of peptide isobars: a record for molecular mass resolution. Anal. Chem. **73**(3), 647–650 (2001)
33. Brustkern, A.M., Rempel, D.L., Gross, M.L.: Ion behavior in an electrically compensated ion cyclotron resonance trap. Int. J. Mass Spectrom. **300**(2), 143–148 (2011)
34. Senko, M.W.: 1998, IsoPro version 3.1, https://sites.google.com/site/isoproms/
35. Kostyukevich, Y., Kononikhin, A.S., Popov, I.A., Nikolaev, E.N.: Simple atmospheric hydrogen/deuterium exchange method for enumeration of labile hydrogens by electrospray ionization mass spectrometry. Anal. Chem. **85**(11), 5330–5334 (2013)
36. Kostyukevich, Y., Kononikhin, A., Popov, I., Kharybin, O., Perminova, I., Konstantinov, A., Nikolaev, E.: Enumeration of labile hydrogens in natural organic matter by use of hydrogen/deuterium exchange Fourier transform ion cyclotron resonance mass spectrometry. Anal. Chem. **85**(22), 11007–11013 (2013)